

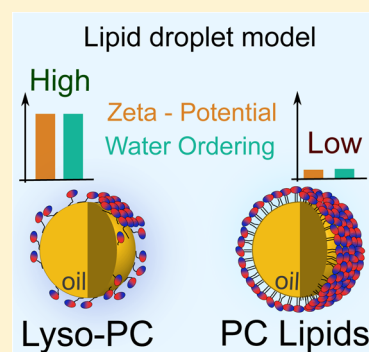
# Interfacial Structure and Hydration of 3D Lipid Monolayers in Aqueous Solution

Halil I. Okur,<sup>1</sup> Yixing Chen, Nikolay Smolentsev, Evangelia Zdrali, and Sylvie Roke\*<sup>1</sup>

Laboratory for Fundamental BioPhotonics (LBP), Institute of Bioengineering (IBI), and Institute of Materials Science (IMX), School of Engineering (STI), and Lausanne Centre for Ultrafast Science (LACUS), École Polytechnique Fédérale de Lausanne (EPFL), CH-1015 Lausanne, Switzerland

## Supporting Information

**ABSTRACT:** Three-dimensional (3D) phospholipid monolayers at hydrophobic surfaces are ubiquitous and found in nature as adiposome organelles or in man-made materials such as drug delivery systems. However, the molecular level understanding of such monolayers remains elusive. Here, we investigate the molecular structure of phosphatidylcholine (PC) lipids forming 3D monolayers on the surface of hexadecane nanodroplets. The effects of acyl chain length, saturation, and number of acyl tails per lipid were studied with vibrational sum frequency and second harmonic scattering techniques. We find that 1,2-dihexadecanoyl-*sn*-glycero-3-phosphocholine (DPPC) lipids form tightly packed monolayers. Upon shortening the tail length to 1,2-dimyristoyl-*sn*-glycero-3-phosphocholine (DMPC) and 1,2-dilauroyl-*sn*-glycero-3-phosphocholine (DLPC), more gauche defects are observed. Monolayers of unsaturated 1,2-dioleoyl-*sn*-glycero-3-phosphocholine (DOPC) and single acyl chained 1-palmitoyl-2-hydroxy-*sn*-glycero-3-phosphocholine (lyso-PC) contain more disorder. Despite these variations in the packing, the headgroup orientation remained approximately parallel to the nanodroplet interface. Remarkably, the lyso-PC uniquely forms more diluted and “patchy” 3D monolayers.



## INTRODUCTION

Phospholipid monolayers are omnipresent in nature and play irreplaceable roles in atmospheric and biological sciences. In living organisms, phospholipid monolayers are found in adiposomes, also known as lipid droplets.<sup>1,2</sup> Lipid droplets have been discovered as organelles that regulate the lipid and fat metabolism in eukaryotic cells. Such organelles are covered by a phospholipid and protein rich monolayer that serves as a regulating barrier between the hydrophobic nonpolar lipid core and aqueous cytosol solution.<sup>1,2</sup> Additionally, phospholipid monolayers on synthetic systems are also of great interest in bioengineering applications and drug delivery.<sup>3</sup> Due to their significant physiological relevance, direct bioengineering impact, and fundamental scientific interests, phospholipid monolayers are widely studied, most often on idealized planar air/water interfaces with a relatively high lateral pressure. On these systems, X-ray and neutron diffraction,<sup>4–8</sup> sum frequency generation,<sup>9–13</sup> Brewster angle<sup>14</sup> and fluorescence<sup>15</sup> microscopies, as well as pressure–area isotherms<sup>13,16</sup> and molecular dynamics (MD) simulations<sup>17–20</sup> have been employed to elucidate the macroscopic and molecular level properties of lipid monolayers. Although phospholipid monolayers at the air/water interface resemble the structures found in the alveoli,<sup>19,21</sup> the findings of these reports cannot be directly applied to processes occurring at the buried nanoscopic hydrophobic/aqueous solution interfaces that one finds in adiposomes and lipid bilayer membranes. A liquid nanometric hydrophobic phase will alter lipid interactions and/or lipid packing. As such,

phospholipid monolayers at hydrophobic/water interfaces should systematically be investigated.

Herein, we utilize hexadecane nanodroplets as a model system for adiposomes and study the structure and conformation of zwitterionic phosphatidylcholine (PC, see Figure 1A for chemical structure) lipids, with different tail length, saturation, and number of tails, as these are the most abundant lipids in cell membranes and at the surface of lipid droplets.<sup>22</sup> A combination of vibrational sum frequency scattering (SFS) spectroscopy and second harmonic scattering (SHS) is used to probe both the lipid headgroup and tail regions along with the orientational order of hydrating water molecules around the lipid head groups in these 3D lipid monolayer systems.

Sum frequency generation (SFG) is a vibrational coherent spectroscopy that measures the combined infrared and Raman spectrum of molecules in noncentrosymmetric environments, such as interfaces.<sup>23,24</sup> Combining SFG with light scattering, SFS, provides molecular level information on nano- and microscopic droplet and particle interfaces by probing the vibrational spectrum of interfacial molecules.<sup>25,26</sup> Due to the inherent sensitivity to noncentrosymmetry, the alkyl chain conformation of the interfacial molecules can be probed by the amplitude ratio of the symmetric (*s*)-CH<sub>2</sub> stretch (*d*<sup>+</sup>) and the

Received: January 19, 2017

Revised: February 27, 2017

Published: March 6, 2017

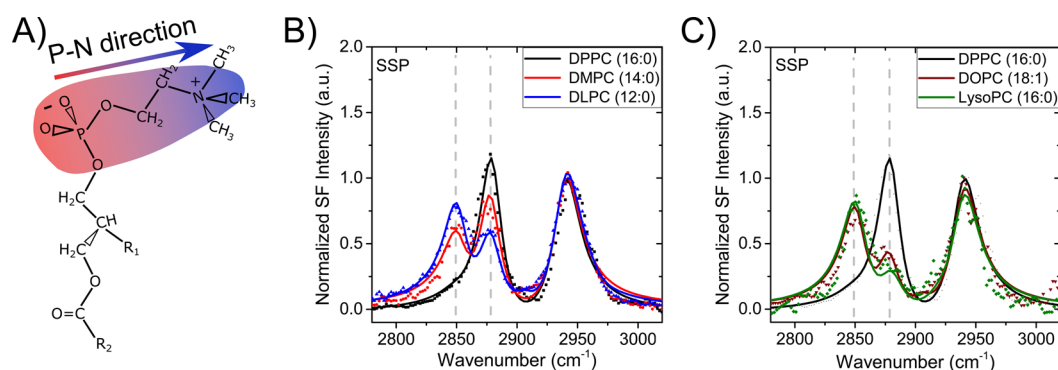


**Figure 1.** The effect of tail length on the lipid structure in a 3D monolayer. (A) The structure of phospholipids with PC headgroups. The lipid tail groups are denoted as  $R_1$  and  $R_2$  and varied for different PC lipids.  $R_1$  is an  $-\text{OH}$  group for lyso-PC, and for all other lipids,  $R_1$  refers to  $-\text{O}-\text{CO}-$ ,  $R_2$ . The lipid headgroup is a zwitterion. The P–N direction is indicated. (B) SFS spectra in the C–H stretch region of 3D lipid monolayers on 2 vol %  $d_{34}$ -hexadecane nanodroplets in  $\text{D}_2\text{O}$  with 1 mM lipids of DPPC (black), DMPC (red), and DLPC (blue). The SFS spectra were recorded in the SSP polarization combination (S and P denote the polarization of the light, S - sum frequency, S - visible, and P - infrared). The spectral fits were obtained using the procedure described in ref 34 (see also the Supporting Information for details). The symbols are normalized data points, and the lines denote the fitted spectra. (C) SFS spectra of 3D monolayers of the same nanodroplets with 1 mM DOPC (brown) and 1 mM lyso-PC (green) lipids in the C–H stretch region. Note that the DPPC spectrum is added for a direct comparison.

s-( $\text{CH}_3$ ) stretch ( $r^+$ ) modes ( $d^+/r^+$ ).<sup>27,28</sup> An all-trans alkyl chain conformation gives rise to  $d^+/r^+ \ll 1$ , whereas alkyl chain gauche defects result in  $d^+/r^+ \geq 1$ . SHS is a nonresonant second-order nonlinear optical technique that has been utilized to probe the orientational ordering of interfacial water molecules along the surface normal.<sup>26,29–32</sup> Here, it is employed to probe PC monolayer induced changes in the orientational directionality of the water molecules along the surface normal as compared to bulk water.<sup>33</sup> In what follows, we first report the phospholipid surface structure as a function of acyl tail length, comparing DPPC (16:0; 16 carbon long acyl tails:0 unsaturated bonds), DMPC (14:0), and DLPC (12:0), and the influence of unsaturated bonds at the lipid tails (DOPC (18:1)) as well as the single-tailed lipids (lyso-PC (16:0)) on the molecular structure of lipids at the surface of oil nanodroplets. Then, we show the lipid headgroup hydration and the corresponding  $\text{PO}_2^-$  vibrational resonance spectra of all tested lipids. Finally, we discuss the unique behavior of lyso-PC that forms a diluted and discontinuous monolayer that keeps the hydration shells in contact with the surface of oil nanodroplets.

## RESULTS AND DISCUSSION

Figure 1B displays the SFS spectra of different lipid monolayers on the  $d_{34}$ -hexadecane oil nanodroplet ( $\sim 100$  nm in radius, see Materials and Methods) in  $\text{D}_2\text{O}$ . The C–H stretch band region ( $2800\text{--}3000$   $\text{cm}^{-1}$ ) is measured for solutions containing 1 mM DPPC, DMPC, or DLPC lipids. (1 mM lipid concentration was recently shown to form a saturated 3D monolayer for DPPC lipids.<sup>33</sup>) The spectra are composed of the symmetric (s)- $\text{CH}_2$  stretch ( $\sim 2850$   $\text{cm}^{-1}$ ,  $d^+$ ), the s- $\text{CH}_3$  stretch ( $\sim 2879$   $\text{cm}^{-1}$ ,  $r^+$ ), and the antisymmetric (as)- $\text{CH}_3$  stretch ( $\sim 2965$   $\text{cm}^{-1}$ ,  $r^-$ ) vibrational modes, along with the s- $\text{CH}_2$ -Fermi resonance ( $\sim 2905$   $\text{cm}^{-1}$ ,  $d^+_{\text{FR}}$ ), the s- $\text{CH}_3$ -Fermi resonance ( $\sim 2937$   $\text{cm}^{-1}$ ,  $r^+_{\text{FR}}$ ), and the as- $\text{CH}_2$  stretch modes ( $\sim 2919$   $\text{cm}^{-1}$ ,  $d^-$ ). The 3D monolayer of DPPC lipids was recently characterized. A liquid condensed-like monolayer with acyl chains in an all-trans conformation was shown to be formed for a 1 mM lipid concentration, with a projected molecular surface area of  $\sim 48$   $\text{\AA}^2$  per lipid.<sup>33</sup> As can be seen from the figure, a different chemical structure of the lipids gives rise to a change in the

intensities of the s- $\text{CH}_2$  stretch ( $d^+$ ) and s- $\text{CH}_3$  stretch ( $r^+$ ) modes, whereas the other vibrational resonances remain almost the same. From DPPC to DLPC, the  $d^+$  peak gradually increases in intensity, while the  $r^+$  resonance gradually loses some intensity as the acyl tails become shorter in length. The  $d^+/r^+$  amplitude ratios are  $\sim 0.0 \pm 0.2$  for DPPC (the same as in ref 33),  $0.6 \pm 0.2$  for DMPC, and  $1.15 \pm 0.2$  for DLPC. This change suggests that the degree of gauche defects in the phospholipid monolayer increases with a decrease in the tail length. Interestingly, almost two decades ago, the completely reversed trend—that shortening lipid acyl tails decreases the amount of gauche defects—was shown for the monolayers of the very same lipids at the planar carbon tetrachloride ( $\text{CCl}_4$ )/ $\text{H}_2\text{O}$  interface.<sup>35,36</sup> The discrepancy arises because  $\text{CCl}_4$  can penetrate the acyl tail groups of the lipid monolayer, as it is a small hydrophobic molecule. This will promote the presence of gauche defects and more so for longer acyl tail lipids than shorter ones. In sharp contrast, hexadecane molecules do not display the same behavior. Indeed, the DPPC monolayers are shown to only slightly disturb the hexadecane oil phase.<sup>33</sup> Furthermore, 3D monolayers have molecular structures that are slightly different compared to planar interfaces.<sup>33</sup>

Physiologically relevant lipid monolayers consist of many more types of lipids that are both saturated and unsaturated. As lipid droplets are a hub for lipid metabolism,<sup>37</sup> unsaturated lipids as well as single-tailed lipid metabolites are also present in the interfacial region.<sup>22</sup> Figure 1C shows SFS spectra of the C–H-stretch modes of 1 mM DOPC and 1 mM lyso-PC lipids on the  $d_{34}$ -hexadecane nanodroplets in  $\text{D}_2\text{O}$ . The same above-mentioned vibrational resonances are present in the spectra. The  $d^+$  mode appears to be the dominant vibrational resonance compared to the  $r^+$  mode in both spectra. The respective  $d^+/r^+$  ratios are  $1.5 \pm 0.2$  and  $2.3 \pm 0.2$  for DOPC and lyso-PC, respectively. Compared to two-tailed fully saturated lipids, these larger  $d^+/r^+$  values indicate even more gauche defects and thus more disordered, liquid condensed/liquid expanded like monolayers. Such disordered monolayers should form with DOPC lipids due to the presence of methylene groups in each acyl tail. It has been shown that experimentally probing unsaturated lipids at planar interfaces in their natural form is quite challenging.<sup>38</sup> Here, however, the DOPC molecules at the nanodroplet/aqueous solution interfaces are buried under

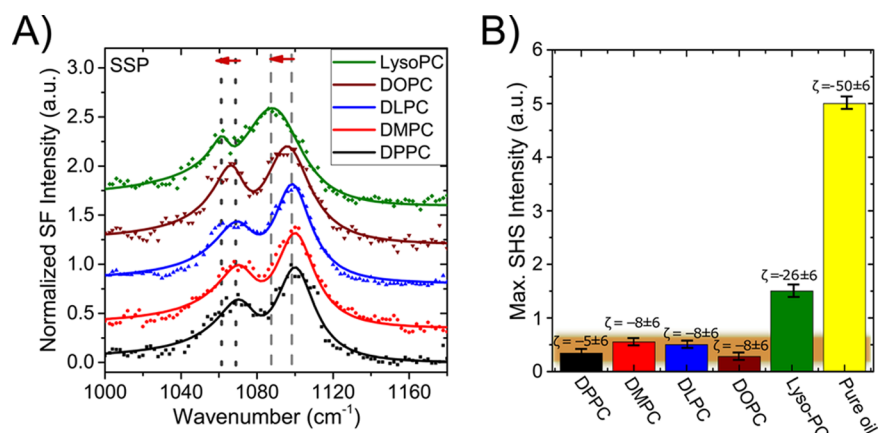


**Figure 2.** Phosphatidylcholine (PC) lipid headgroup structure. (A) SFS spectra taken in the P–O stretch region of 3D monolayers on 2 vol %  $d_{34}$ -hexadecane nanodroplets in  $D_2O$  with 1 mM lipids involving DPPC (black), DMPC (red), DLPC (blue), DOPC (brown), and lyso-PC (green). The spectra are offset for clarity. The SFS spectra were recorded in the SSP polarization combination. The symbols are normalized data points, and the lines indicate the fitted spectra. The dashed (gray) lines denote the  $s\text{-PO}_2^-$  stretch peak positions, and the dotted (black) lines show the  $s\text{-CO-O-C}$  stretch peak positions. The red arrows indicate the red shifts for lyso-PC lipids compared to other tested lipids. (B) The SHS intensities and  $\zeta$ -potential values of 3D monolayers consisting of DPPC (black), DMPC (red), DLPC (blue), DOPC (brown), and lyso-PC (green) lipids along with pure hexadecane oil droplets (yellow) are plotted. The data report the SHS intensity in the PPP polarization combination at the scattering angle ( $35\text{--}45^\circ$ ), that gives rise to the maximum intensity. The orange highlighted region shows that the SHS intensity reaches low values for all double-tailed lipid samples.

water and presumably well-preserved from common reactive oxygen species. As such, our reported DOPC spectrum can serve as a good reference for future unsaturated lipid studies. Additionally, the large  $d^+/r^+$  ratio for lyso-PC results from the altered aspect ratio between the PC headgroup and acyl tail region. One can argue that such sizable differences in the tail region  $d^+/r^+$  ratios from  $\sim 0$  to  $\sim 2.3$  should also influence the lipid headgroup structure. The  $s\text{-PO}_2^-$  stretch peak has been widely employed to probe the lipid headgroup orientation and the H-bonding environment of the hydrated phospholipid headgroup.<sup>39,40</sup> As such, in what follows, we focus on the spectral region of  $1000\text{--}1180\text{ cm}^{-1}$  to probe the  $s\text{-PO}_2^-$  stretch mode of the lipids.

Figure 2A shows the SFS spectra of 3D monolayers of DPPC, DMPC, DLPC, DOPC, and lyso-PC lipids recorded in the phosphate stretch region. Two main spectral features at  $\sim 1070$  and  $\sim 1100\text{ cm}^{-1}$  are observed and assigned to  $s\text{-CO-O-C}$  stretch and  $s\text{-PO}_2^-$  stretch modes for all tested lipids, respectively. Such peak assignments agree with previous reports.<sup>33,40,41</sup> The  $s\text{-PO}_2^-$  band at  $1100\text{ cm}^{-1}$  is apparent for all tested lipid samples, but the same vibrational resonance arises at around  $1090\text{ cm}^{-1}$  with a larger bandwidth for lyso-PC (green curve). Moreover, the  $s\text{-CO-O-C}$  band of lyso-PC also red shifts by  $\sim 8\text{ cm}^{-1}$ . Such peak shifts in the SFS spectrum indicate that the lyso-PC lipids in the 3D monolayers experience somewhat different interactions and a different hydration environment compared to other PC lipids. In analogy to previous observations,<sup>39,40</sup> a  $\sim 10\text{ cm}^{-1}$  red shift is a clear indication of a more H-bond donor rich hydration environment around the lyso-PC headgroup. The red shift in the  $s\text{-CO-O-C}$  stretch peak can also be understood as arising from a stronger H-bond donating hydration environment.<sup>42,43</sup> That these  $\text{PO}_2^-$  and  $\text{CO-O-C}$  stretch modes are shifted and widened suggests that not only the PC headgroup but also the glycerol group of the lipids are well hydrated. Thus, for monolayers consisting of the lyso-PC lipids, the hydrating water molecules can penetrate further in between lipid molecules. In order to further investigate the hydration environment and the

possible differences between lyso-PC and the other lipids, we probe the 3D lipid monolayers with SHS measurements. The SHS intensity reports on the orientational directionality of water molecules along the surface normal in the interfacial region.<sup>26,29,44</sup>

Figure 2B shows the SHS intensity of 3D monolayers with 1 mM DPPC, DMPC, DLPC, DOPC, and lyso-PC lipids on hexadecane nanodroplets as well as bare hexadecane nanodroplets in water. The 3D DPPC, DMPC, DLPC, and DOPC monolayers all exhibit low SHS intensities ( $<0.55$ , highlighted by the orange area in Figure 2b). Thus, these monolayers have a small influence on the orientational order of water molecules in the interfacial region. The same samples also yield negative but small zeta-potential values, obtained from electrokinetic mobility measurements (from  $-5 \pm 6$  to  $-8 \pm 6\text{ mV}$ ). The PC headgroups are known to interact strongly with water,<sup>45,46</sup> but the charged phosphate and choline residues each orient water in opposite directions.<sup>47,48</sup> The lack of any significant SHS intensity strongly suggests that the interfacial water molecules align parallel to the nanodroplet surface on average, with a minimum orientational order contribution toward the surface normal, at least for fully covered monolayers. This water alignment can only occur when the above-mentioned lipid headgroup (P–N direction) orientation is preferentially away from the surface normal. Such a lipid headgroup orientation agrees with recent literature.<sup>16,33</sup> In contrast, the bare oil droplets (yellow bar), that are not covered with a monolayer, show significant SHS intensity and are negatively charged ( $-50 \pm 6\text{ mV}$ , see also ref 49). Note that, although these results have been reproduced numerous times, no satisfactory explanation has been given for the origin of the negative charge.<sup>50</sup> Nonetheless, charge induced orientational ordering in the interfacial water layer has been demonstrated<sup>31,32</sup> (with H atoms of water pointing primarily toward the surface),<sup>51</sup> and here we measure the same behavior for the bare hexadecane oil droplets.

Interestingly, the lyso-PC lipids show an intermediate behavior: A significantly higher ( $\sim 3\times$ ) SHS intensity (green

bar) that suggests substantial enhancement in the interfacial water ordering as well as a more negative ( $-26 \pm 6$  mV)  $\zeta$ -potential value than the other PC monolayers are measured. In addition to these SHS and  $\zeta$ -potential variations, the red shifts in the  $s\text{-PO}_2^-$  and  $s\text{-CO-OC}$  stretch modes reflect a different headgroup hydrating environment. These are rather unexpected results. One can argue that a more diluted lyso-PC monolayer with lower lipid number density potentially leaves some bare hexadecane surface in direct contact with interfacial water molecules. This would result in a high  $\zeta$ -potential and high SHS signal intensity by the phenomenological negative charge at the bare oil surface. To test this hypothesis, we compared the SFS spectral amplitude of the C–H stretch region ( $2800\text{--}3000\text{ cm}^{-1}$ ) for lyso-PC and DLPC 3D monolayers to estimate the relative lipid number density (also taking the number of lipid tail differences into account). Here, a DLPC monolayer serves as a good reference, since it yields a similar  $d^+/r^+$  ratio as lyso-PC lipids while fully covering the oil surface, evident by the very low SHS signal and small zeta potential values. An overall  $\sim 35\%$  decrease is observed for the total number of lipids in the phospholipid monolayer for lyso-PC compared to the DLPC (see Figure S1 and section S2 for further discussion). Such a decrease in the total number of lipids clearly indicates that there is an insufficient amount of lyso-PC lipids on the surface to cover the entire hydrophobic oil surface, in agreement with the proposed hypothesis. The resultant structures are illustrated in Figure 3. Note that the tested lipid concentration is

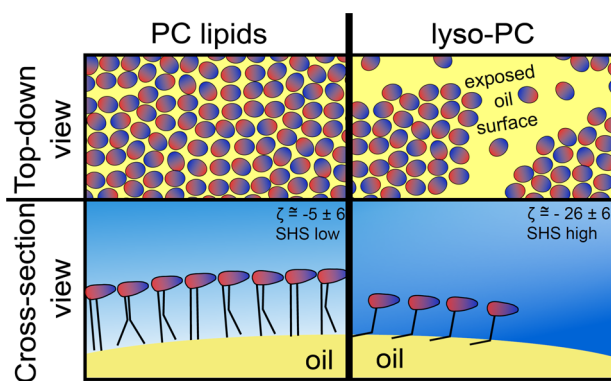


**Figure 3.** Proposed molecular picture. The schematics show the top-down (top) and cross-section (bottom) views of a section of a single nanodroplet. The left panels illustrate all of the double-tailed PC lipids including DPPC, DMPC, DLPC, and DOPC that form a fully saturated phospholipid monolayer. The right panels illustrate the discontinuous phospholipid monolayer formed by the lyso-PC.

substantially above the critical micelle concentration (cmc) of lyso-PC ( $\sim 140 \times$  cmc) in the sample solution. As a consequence, there are more than enough lipid molecules in the aqueous solution to cover the entire nanodroplet surface (while micelles do not contribute to the SFS response<sup>52</sup>). As such, the discontinuous 3D monolayers are in equilibrium with the aqueous solution.

On the basis of these results, it is clear that the single-tailed lipids demonstrate more gauche defects than the double-tailed lipids (Figure 1) and introduce some degree of discontinuity in the lipid monolayer which results in bigger hydration shells around the lipid head groups (Figure 2A). They also substantially alter the orientation order of the interfacial hydration environment by forming a discontinuous monolayer (Figure 2B). Single-tailed lipids are important and significant

constituents of the surface of naturally occurring lipid droplets in eukaryotic cells.<sup>22</sup> They (including lyso-PC) serve as diluting agents in the phospholipid monolayer and possibly mediate the accessibility to the nonpolar cores, i.e., the insertion and lateral diffusion of perilipin protein (also known as lipid-droplet-associated protein) or access of water-soluble enzymes.<sup>37</sup>

## CONCLUSIONS

In summary, we measured the molecular structure of 3D monolayers consisting of zwitterionic PC lipids including DPPC, DMPC, DLPC, DOPC, and lyso-PC on hexadecane nanodroplets using SFS and SHS. All tested saturated lipids with shorter acyl tails than the DPPC display some gauche defects in the acyl tail region. The degree of order in the acyl tail is reduced for decreasing tail lengths and by introducing unsaturated methylene bonds. Interestingly, this trend reverses at hydrophobic/aqueous interfaces in which the hydrophobic phase consists of small organic molecules, i.e.,  $\text{CCl}_4$ . Nevertheless, these alterations in the lipid tails appear to not influence the lipid headgroup orientation along with the orientational order of water molecules at the 3D monolayer hydration. It is worth noting that the presented DOPC spectra can serve as a benchmark for the molecular structure of unsaturated lipids at the hydrophobic/aqueous interface. Moreover, lyso-PC lipids show some unique properties in 3D monolayers. Such lipids yield an enhanced orientational ordering of interfacial water molecules via forming a discontinuous monolayer that keeps the oil core in contact with interfacial water molecules. These observations were evident from the zeta potential measurements and SHS signal intensity as well as the peak position and bandwidth of the  $s\text{-PO}_2^-$  stretch band. Our findings increase the fundamental understanding of phospholipid monolayers at hydrophobic/aqueous (liquid/liquid) interfaces. That enables the design of new applied soft materials involving nanoscopic 3D monolayers such as drug delivery systems. More importantly, this work sheds some light on the functioning of physiological 3D lipid monolayers, i.e., lipid droplets that help to paint a full molecular picture of the biophysics of lipid monolayers.

## MATERIALS AND METHODS

**Chemicals.** Chemicals were used as received. Hexadecane ( $\text{C}_{16}\text{H}_{34}$ , 99.8%, Sigma-Aldrich),  $d_{34}$ -hexadecane ( $\text{C}_{16}\text{D}_{34}$ , 98% d, Cambridge Isotope), 1,2-dihexadecanoyl-*sn*-glycero-3-phosphocholine (DPPC, 99%, Avanti), 1,2-dimyristoyl-*sn*-glycero-3-phosphocholine (DMPC, 99%, Avanti), 1,2-dilauroyl-*sn*-glycero-3-phosphocholine (DLPC, 99%, Avanti), 1,2-dioleoyl-*sn*-glycero-3-phosphocholine (DOPC, 99%, Avanti), as well as 1-palmitoyl-2-hydroxy-*sn*-glycero-3-phosphocholine (lyso-PC, 99%, Avanti) were used as received. All aqueous solutions were prepared with ultrapure water ( $\text{H}_2\text{O}$ , Milli-Q UF plus, Millipore, Inc., electrical resistance of  $18.2\text{ M}\Omega\cdot\text{cm}$ ) and  $\text{D}_2\text{O}$  (99.8% Armar). All sample solutions were prepared and stored in glassware that was first cleaned with a 1:3  $\text{H}_2\text{O}_2\text{:H}_2\text{SO}_4$  solution, after which it was thoroughly rinsed with a copious amount of ultrapure water.

**3D Lipid Monolayers on Nanodroplets.** Three-dimensional lipid monolayers on nanodroplets in aqueous solution were prepared with 2 v/v % *n*-hexadecane in  $\text{H}_2\text{O}$  (for SHS) or 2 v/v %  $d_{34}$ -hexadecane in  $\text{D}_2\text{O}$  (for SFS) and 1 mM of the preferred PC lipid according to the procedure described in refs 33 and 40. Briefly, the solutions were mixed with a hand-held

homogenizer (TH, OMNI International) for 4 min above the gel phase transition temperature of the chosen lipids. Then, the sample solution was treated with an ultrasonic bath (35 kHz, 400 W, Bandelin) for the same duration. The resultant droplet system was used as is for SFS measurements. It was diluted to 0.1 v/v % with ultrapure water for SHS measurements. The size distribution and zeta-potential of the nanodroplets were measured by dynamic light scattering and electrokinetic mobility measurements (Malvern ZS nanosizer), respectively. A general protocol for these measurements can be found elsewhere.<sup>52</sup> The nanodroplets used in this study had a mean hydrodynamic diameter in the range 180–210 nm with a polydispersity index (PDI) of less than 0.15. Specifically, the diameters of the nanodroplets containing the 3D monolayers prepared with DPPC, DMPC, DLPC, DOPC, and lyso-PC were respectively 185, 210, 202, 180, and 198 nm. The hydrodynamic diameters were calculated from the intensity autocorrelation function with the optical parameters of the materials taken from reference literature.

The stability of the nanodroplets was also investigated. The bare oil droplets were stable over a time span of 1 or 2 days, while the nanodroplets covered with the lipid monolayers displayed a stability of at least several weeks if not a few months. Nevertheless, all presented data was measured from samples that were freshly prepared and were kept in sealed cuvettes before and during the measurements. The entire measurement procedure, including the sample preparation and the SFS and SHS measurements, was performed in the time frame of a day. Throughout this time, the sample solutions were kept at ambient temperature,  $23.5 \pm 0.5$  °C.

## ■ ASSOCIATED CONTENT

### Supporting Information

The Supporting Information is available free of charge on the ACS Publications website at DOI: 10.1021/acs.jpcc.7b00609.

A description of the SFS/SHS measurements and SFS spectral fitting protocols and the estimation of lipid coverage on the surface of nanodroplets, as well as Figure S1 and Tables S1 and S2 (PDF)

## ■ AUTHOR INFORMATION

### Corresponding Author

\*E-mail: sylvie.roke@epfl.ch.

### ORCID

Halil I. Okur: 0000-0002-2492-1168

Sylvie Roke: 0000-0002-6062-7871

### Notes

The authors declare no competing financial interest.

## ■ ACKNOWLEDGMENTS

This work is supported by the Julia Jacobi Foundation and the European Research Council (grant number 616305). We thank Dr. Kailash C. Jena for his contributions to experiments in the early stages of this project.

## ■ REFERENCES

(1) Tauchi-Sato, K.; Ozeki, S.; Houjou, T.; Taguchi, R.; Fujimoto, T. The Surface of Lipid Droplets Is a Phospholipid Monolayer with a Unique Fatty Acid Composition. *J. Biol. Chem.* **2002**, *277*, 44507–44512.

(2) Thiam, A. R.; Farese, R. V., Jr; Walther, T. C. The Biophysics and Cell Biology of Lipid Droplets. *Nat. Rev. Mol. Cell Biol.* **2013**, *14*, 775–786.

(3) Müller, R. H.; Mäder, K.; Gohla, S. Solid Lipid Nanoparticles (SLN) for Controlled Drug Delivery – a Review of the State of the Art. *Eur. J. Pharm. Biopharm.* **2000**, *50*, 161–177.

(4) Kaganer, V. M.; Mowald, H.; Dutta, P. Structure and Phase Transitions in Langmuir Monolayers. *Rev. Mod. Phys.* **1999**, *71*, 779–819.

(5) Schalke, M.; Lösche, M. Structural Models of Lipid Surface Monolayers from X-Ray and Neutron Reflectivity Measurements. *Adv. Colloid Interface Sci.* **2000**, *88*, 243–274.

(6) Krueger, S. Neutron Reflection from Interfaces with Biological and Biomimetic Materials. *Curr. Opin. Colloid Interface Sci.* **2001**, *6*, 111–117.

(7) Kollmitzer, B.; Heftberger, P.; Rappolt, M.; Pabst, G. Monolayer Spontaneous Curvature of Raft-Forming Membrane Lipids. *Soft Matter* **2013**, *9*, 10877–10884.

(8) Harroun, T. A.; Kucerka, N.; Nieh, M.-P.; Katsaras, J. Neutron and X-Ray Scattering for Biophysics and Biotechnology: Examples of Self-Assembled Lipid Systems. *Soft Matter* **2009**, *5*, 2694–2703.

(9) Roke, S.; Schins, J. M.; Müller, M.; Bonn, M. Vibrational Spectroscopic Investigation of the Phase Diagram of a Biomimetic Lipid Monolayer. *Phys. Rev. Lett.* **2003**, *90*, 128101–128101.

(10) Bonn, M.; Roke, S.; Berg, O.; Juurlink, L. B. F.; Stamouli, A.; Muller, M. A Molecular View of Cholesterol-Induced Condensation in a Lipid Monolayer. *J. Phys. Chem. B* **2004**, *108*, 19083–19085.

(11) Watry, M. R.; Tarbuck, T. L.; Richmond, G. L. Vibrational Sum-Frequency Studies of a Series of Phospholipid Monolayers and the Associated Water Structure at the Vapor/Water Interface. *J. Phys. Chem. B* **2003**, *107*, 512–518.

(12) Liljeblad, J. D. F.; Bulone, V.; Tyrode, E.; Rutland, M. W.; Johnson, C. M. Phospholipid Monolayers Probed by Vibrational Sum Frequency Spectroscopy: Instability of Unsaturated Phospholipids. *Biophys. J.* **2010**, *98*, L50–L52.

(13) Liu, W.; Wang, Z.; Fu, L.; Leblanc, R. M.; Yan, E. C. Y. Lipid Compositions Modulate Fluidity and Stability of Bilayers: Characterization by Surface Pressure and Sum Frequency Generation Spectroscopy. *Langmuir* **2013**, *29*, 15022–15031.

(14) Hoenig, D.; Moebius, D. Direct Visualization of Monolayers at the Air-Water Interface by Brewster Angle Microscopy. *J. Phys. Chem.* **1991**, *95*, 4590–4592.

(15) McConnell, H. M. Structures and Transitions in Lipid Monolayers at the Air-Water Interface. *Annu. Rev. Phys. Chem.* **1991**, *42*, 171–195.

(16) Duncan, S. L.; Larson, R. G. Comparing Experimental and Simulated Pressure-Area Isotherms for Dppc. *Biophys. J.* **2008**, *94*, 2965–2986.

(17) Dominguez, H.; Smondyrev, A. M.; Berkowitz, M. L. Computer Simulations of Phosphatidylcholine Monolayers at Air/Water and Ccl4/Water Interfaces. *J. Phys. Chem. B* **1999**, *103*, 9582–9588.

(18) Shinoda, W.; DeVane, R.; Klein, M. L. Zwitterionic Lipid Assemblies: Molecular Dynamics Studies of Monolayers, Bilayers, and Vesicles Using a New Coarse Grain Force Field. *J. Phys. Chem. B* **2010**, *114*, 6836–6849.

(19) Rose, D.; Rendell, J.; Lee, D.; Nag, K.; Booth, V. Molecular Dynamics Simulations of Lung Surfactant Lipid Monolayers. *Biophys. Chem.* **2008**, *138*, 67–77.

(20) Kaznessis, Y. N.; Kim, S.; Larson, R. G. Simulations of Zwitterionic and Anionic Phospholipid Monolayers. *Biophys. J.* **2002**, *82*, 1731–1742.

(21) Ma, G.; Allen, H. C. Real-Time Investigation of Lung Surfactant Respreading with Surface Vibrational Spectroscopy. *Langmuir* **2006**, *22*, 11267–11274.

(22) Bartz, R.; Li, W.-H.; Venables, B.; Zehmer, J. K.; Roth, M. R.; Welti, R.; Anderson, R. G. W.; Liu, P.; Chapman, K. D. Lipidomics Reveals That Adiposomes Store Ether Lipids and Mediate Phospholipid Traffic. *J. Lipid Res.* **2007**, *48*, 837–847.

- (23) Shen, Y. R. Surface Properties Probed by Second-Harmonic and Sum-Frequency Generation. *Nature* **1989**, *337*, 519–519.
- (24) Harris, A. L.; Chidsey, C. E. D.; Levinos, N. J.; Loiacono, D. N. Monolayer Vibrational Spectroscopy by Infrared-Visible Sum Generation at Metal and Semiconductor Surfaces. *Chem. Phys. Lett.* **1987**, *141*, 350–356.
- (25) Roke, S.; Roeterdink, W. G.; Wijnhoven, J. E. G. J.; Petukhov, A. V.; Kleyn, A. W.; Bonn, M. Vibrational Sum Frequency Scattering from a Sub-Micron Suspension. *Phys. Rev. Lett.* **2003**, *91*, 258302–258302.
- (26) Roke, S.; Gonella, G. Nonlinear Light Scattering and Spectroscopy of Particles and Droplets in Liquids. *Annu. Rev. Phys. Chem.* **2012**, *63*, 353–378.
- (27) Guyot-Sionnest, P.; Hunt, J. H.; Shen, Y. R. Sum-Frequency Vibrational Spectroscopy of a Langmuir Film: Study of Molecular-Orientation of a Two-Dimensional System. *Phys. Rev. Lett.* **1987**, *59*, 1597–1600.
- (28) Tyrode, E.; Hedberg, J. A Comparative Study of the Cd and Ch Stretching Spectral Regions of Typical Surfactants Systems Using Vsfs: Orientation Analysis of the Terminal Ch3 and Cd3 Groups. *J. Phys. Chem. C* **2012**, *116*, 1080–1091.
- (29) Ong, S.; Zhao, X.; Eisenthal, K. B. Polarization of Water Molecules at a Charged Interface: Second Harmonic Studies of the Silica/Water Interface. *Chem. Phys. Lett.* **1992**, *191*, 327–335.
- (30) Schürer, B.; Wunderlich, S.; Sauerbeck, C.; Peschel, U.; Peukert, W. Probing Colloidal Interfaces by Angle-Resolved Second Harmonic Light Scattering. *Phys. Rev. B: Condens. Matter Mater. Phys.* **2010**, *82*, 241404–241404.
- (31) Scheu, R.; Rankin, B. M.; Chen, Y.; Jena, K. C.; Ben-Amotz, D.; Roke, S. Charge Asymmetry at Aqueous Hydrophobic Interfaces and Hydration Shells. *Angew. Chem., Int. Ed.* **2014**, *53*, 9560–9563.
- (32) Scheu, R.; Chen, Y.; de Aguiar, H. B.; Rankin, B. M.; Ben-Amotz, D.; Roke, S. Specific Ion Effects in Amphiphile Hydration and Interface Stabilization. *J. Am. Chem. Soc.* **2014**, *136*, 2040–2047.
- (33) Chen, Y.; Jena, K. C.; Lütgebaucks, C.; Okur, H. I.; Roke, S. Three Dimensional Nano “Langmuir Trough” for Lipid Studies. *Nano Lett.* **2015**, *15*, 5558–5563.
- (34) de Aguiar, H. B.; Strader, M. L.; de Beer, A. G. F.; Roke, S. Surface Structure of Sds Surfactant and Oil at the Oil-in-Water Droplet Liquid/Liquid Interface: A Manifestation of a Non-Equilibrium Surface State. *J. Phys. Chem. B* **2011**, *115*, 2970–2978.
- (35) Walker, R. A.; Conboy, J. C.; Richmond, G. L. Molecular Structure and Ordering of Phospholipids at a Liquid-Liquid Interface. *Langmuir* **1997**, *13*, 3070–3073.
- (36) Walker, R. A.; Gruetzmacher, J. A.; Richmond, G. L. Phosphatidylcholine Monolayer Structure at a Liquid-Liquid Interface. *J. Am. Chem. Soc.* **1998**, *120*, 6991–7003.
- (37) Guo, Y.; Cordes, K. R.; Farese, R. V.; Walther, T. C. Lipid Droplets at a Glance. *J. Cell Sci.* **2009**, *122*, 749–752.
- (38) Liljeblad, J. F. D.; Bulone, V.; Tyrode, E.; Rutland, M. W.; Johnson, C. M. Phospholipid Monolayers Probed by Vibrational Sum Frequency Spectroscopy: Instability of Unsaturated Phospholipids. *Biophys. J.* **2010**, *98*, L50–L52.
- (39) Ma, G.; Allen, H. C. Dppc Langmuir Monolayer at the Air-Water Interface: Probing the Tail and Head Groups by Vibrational Sum Frequency Generation Spectroscopy. *Langmuir* **2006**, *22*, 5341–5349.
- (40) Smolentsev, N.; Lütgebaucks, C.; Okur, H. I.; de Beer, A. G. F.; Roke, S. Intermolecular Headgroup Interaction and Hydration as Driving Forces for Lipid Transmembrane Asymmetry. *J. Am. Chem. Soc.* **2016**, *138*, 4053–4060.
- (41) Casillas-Ituarte, N. N.; Chen, X.; Castada, H.; Allen, H. C. Na<sup>+</sup> and Ca<sup>2+</sup> Effect on the Hydration and Orientation of the Phosphate Group of Dppc at Air–Water and Air–Hydrated Silica Interfaces. *J. Phys. Chem. B* **2010**, *114*, 9485–9495.
- (42) Okur, H. I.; Kherb, J.; Cremer, P. S. Cations Bind Only Weakly to Amides in Aqueous Solutions. *J. Am. Chem. Soc.* **2013**, *135*, 5062–5067.
- (43) Tamm, L. K.; Tatulian, S. A. Infrared Spectroscopy of Proteins and Peptides in Lipid Bilayers. *Q. Rev. Biophys.* **1997**, *30*, 365–429.
- (44) Petersen, P. B.; Saykally, R. J. Probing the Interfacial Structure of Aqueous Electrolytes with Femtosecond Second Harmonic Generation Spectroscopy. *J. Phys. Chem. B* **2006**, *110*, 14060–14073.
- (45) Chen, X.; Hua, W.; Huang, Z.; Allen, H. C. Interfacial Water Structure Associated with Phospholipid Membranes Studied by Phase-Sensitive Vibrational Sum Frequency Generation Spectroscopy. *J. Am. Chem. Soc.* **2010**, *132*, 11336–11342.
- (46) Kim, J.; Kim, G.; Cremer, P. S. Investigations of Water Structure at the Solid/Liquid Interface in the Presence of Supported Lipid Bilayers by Vibrational Sum Frequency Spectroscopy. *Langmuir* **2001**, *17*, 7255–7260.
- (47) Mondal, J. A.; Nihonyanagi, S.; Yamaguchi, S.; Tahara, T. Three Distinct Water Structures at a Zwitterionic Lipid/Water Interface Revealed by Heterodyne-Detected Vibrational Sum Frequency Generation. *J. Am. Chem. Soc.* **2012**, *134*, 7842–7850.
- (48) Mondal, J. A. Effect of Trimethylamine N-Oxide on Interfacial Electrostatics at Phospholipid Monolayer–Water Interfaces and Its Relevance to Cardiovascular Disease. *J. Phys. Chem. Lett.* **2016**, *7*, 1704–1708.
- (49) Vácha, R.; Rick, S. W.; Jungwirth, P.; de Beer, A. G. F.; de Aguiar, H. B.; Samson, J. S.; Roke, S. The Orientation and Charge of Water at the Hydrophobic Oil Droplet-Water Interface. *J. Am. Chem. Soc.* **2011**, *133*, 10204–10210.
- (50) Agmon, N.; Bakker, H. J.; Campen, R. K.; Henschman, R. H.; Pohl, P.; Roke, S.; Thämer, M.; Hassanali, A. Protons and Hydroxide Ions in Aqueous Systems. *Chem. Rev.* **2016**, *116*, 7642–7672.
- (51) Lütgebaucks, C.; Gonella, G.; Roke, S. Optical Label-Free and Model-Free Probe of the Surface Potential of Nanoscale and Microscopic Objects in Aqueous Solution. *Phys. Rev. B: Condens. Matter Mater. Phys.* **2016**, *94*, 195410.
- (52) Aguiar, H. B. d.; Beer, A. G. F. d.; Strader, M. L.; Roke, S. The Interfacial Tension of Nanoscopic Oil Droplets in Water Is Hardly Affected by Sds Surfactant. *J. Am. Chem. Soc.* **2010**, *132*, 2122–2123.